Sensors & Actuators: B. Chemical 273 (2018) 350–357

Contents lists available at ScienceDirect

Sensors and Actuators B: Chemical

journal homepage: www.elsevier.com/locate/snb

Self-powered disposable prothrombin time measurement device with an integrated effervescent pump

Mustafa Tahsin Guler[a], Ziya Isiksacan[b], Murat Serhatlioglu[b], Caglar Elbuken[b,*]

[a] Department of Physics, Kirikkale University, 71450, Kirikkale, Turkey
[b] UNAM - National Nanotechnology Research Center and Institute of Materials Science and Nanotechnology, Bilkent University, 06800, Ankara, Turkey

ARTICLE INFO

Keywords:
Coagulation
Prothrombin time
Microfluidics
Chemical pump
Point-Of-Care
3D printing

ABSTRACT

Coagulation is an essential physiological activity initiated by the interaction of blood components for clot formation. Prothrombin time (PT) measurement is a clinical test for the assessment of the extrinsic/common pathways of coagulation cascade. Periodic measurement of PT is required under numerous conditions including cardiovascular disorders. We present a self-powered microfluidic device for quantitative PT measurement from 50 µl whole blood. The entire platform is disposable and does not require any external pumping, power, or readout units. It consists of a 3D-printed effervescent pump for CO_2 generation from a chemical reaction, a cartridge for two-channel fluid flow (blood and water), and a grid for the quantification of fluid migration distance. Following the introduction of the fluids to the corresponding channel inlets, marking the coagulation start, an acid-base reaction is triggered for gas generation that drives the fluids within the channels. When the blood coagulates, its flow in the channel is halted. At that point, the distance water has travelled is measured using the grid. This distance correlates with PT as demonstrated through clinical tests with patient samples. This single-unit device has a potential for rapid evaluation and periodic monitoring of PT in the clinical settings and at the point-of-care.

1. Introduction

Blood coagulation is a dynamic hematological activity necessitating the interplay of numerous plasma proteins, cells, and coagulation factors for the formation of cross-linked fibrin networks to prevent bleeding [1,2]. The coagulation cascade is triggered by either extrinsic or intrinsic pathways through the activation of tissue factors or surface, respectively, and leads to a common pathway where stable fibrin strands are formed from fibrinogen [3,4]. Prothrombin time (PT) test is frequently performed in clinics for the evaluation of the extrinsic and common pathways of the coagulation cascade [5]. Sensitive and periodic measurement of this parameter is critical for patients who are under pre-, peri-, and post- operative monitoring or undertaking anticoagulant therapy for the regulation of the clotting status by the blood-thinning drugs such as a vitamin K antagonist Coumadin® [6,7]. People with coagulation disorders, atrial fibrillation, pulmonary embolism, myocardial infarction, and several other cardiovascular diseases as well as heart valve prosthesis need lifelong anticoagulant therapy [8,9]. However, the medications for the therapy have narrow therapeutic windows [10]. Therefore, the required dose varies among individuals and fluctuates for the same patient on a daily basis because of diet and genetic background [10,11]. The failure to receive maintenance doses may result in either hemorrhage or thrombo-embolism, which are both life-threatening [12,13]. The conventional practice to monitor the course of the therapy is hospital visits at fixed intervals for PT measurements by benchtop devices. This practice, on the other hand, is time-consuming and expensive, and delayed visits may end up with unfortunate consequences.

Point-of-care devices have been developed to address the issues associated with the benchtop counterparts in clinical settings [14]. Commercial coagulation time measurement devices have been launched to decrease the test turnaround times [15]. Different measurement principles are being utilized including electrochemical detection (CoaguChek XS), mechanical measurement by a cantilever (CoagMax), or optical detection of the cease of blood flow (Hemochron Signature) [16,17]. These products consist of a main device and disposable test cartridges that contain the necessary reagents, electrodes, magnetic particles, or MEMS structures depending on the measurement principle. Even though these products have a potential for point-of-care testing to facilitate timely intervention in case of emergency, the costs of the main devices make them unaffordable for the majority. Since the health insurances in most of the countries (including the authors' homeland)

* Corresponding author.
E-mail address: elbuken@unam.bilkent.edu.tr (C. Elbuken).

https://doi.org/10.1016/j.snb.2018.06.042
Received 26 March 2018; Received in revised form 28 May 2018; Accepted 8 June 2018
Available online 15 June 2018
0925-4005/ © 2018 Elsevier B.V. All rights reserved.

have limited coverage for such devices, the patients are dependent on clinics or anticoagulation centers for their periodic PT measurements. The tests are even more inaccessible for those living in resource-poor regions. The microfluidics community is aiming to develop novel methodologies for the PT measurements such as impedimetric [18], aptamer-based [19], paper-based [20], cantilever-based [21], quartz crystal microbalance (QCM) [22], centrifugal [23] and fluorescence-based [24]. These studies, on the other hand, generally have a long way to compactness and lack clinical validation tests, which are necessary for commercialization.

The requirement to employ external components such as pumps, power sources, and control circuitry increases the cost and complexity of lab-on-a-chip platforms while limiting their portability [25]. Miniaturized integration of these components is desired to make these platforms appropriate for point-of-care use [26]. Apart from the frequently used pressure or syringe pumps, the liquid handling is aimed through micropumps categorized as non-mechanical (electrowetting, electrokinetic, electrochemical) and mechanical (rotary, peristaltic, diaphragm) [27,28]. Of the first category, chemical pumps have recently become popular for the construction of self-powered platforms due to their simple fabrication and integration [29]. Examples include the decomposition of H_2O_2 or N_2H_4 in the presence of metal substrates (e.g., Ag, Au, Pt, Pd) for self- electrophoresis [30] or electroosmosis [31], respectively. Methanol is decomposed in a microfluidic device to generate CO_2 for fluid pumping [32]. Differing from this trend, chemical pumps can also be designed without any need for microfabricated substrates. Effervescent tablets used in medical treatment are composed of an acid and a base. Before intake, these tablets are dissolved in water generating CO_2 bubbles. As shown in this work, effervescent micropumps can employ acid-base neutralization reactions in aqueous solutions that generate enough CO_2 for long durations to drive fluids in microfluidic systems for a variety of applications. These effervescent micropumps yield predictable pressures, with rapid response times and long durations at steady-state values, that are firmly controlled by the type and the molarity of the reactants used in the reactions [33].

In this manuscript, we present a portable and entirely disposable microfluidic device for point-of-care PT measurement from 50 µl whole blood in less than 2 min. The device is lightweight (50 g) and does not require any external components. Even though the device is designed for self-evaluation of the test result, integration of a cell phone makes it an ideal telemedicine application if needed. The key element of this self-powered system is an integrated effervescent pump where an acid-base neutralization reaction generates CO_2 gas that supplies pressure for liquid flow within the two-channel test cartridge. The sample channel is for whole blood, whereas the reference channel is for DI water. The assay principle is based on the measurement of the distance travelled by water using an integrated grid upon the cease of the blood flow due to coagulation. We explained the fabrication steps of the 3D-printed effervescent pump and characterization results of the generated pressure and settling time of the pump for different acid and base molarities. Comparative tests were performed at a local clinic using a conventional benchtop device to show the potential of our system for reliable and quantitative PT measurements.

2. Experimental section

2.1. Materials

We obtained ethical approvals from the Ethics Committees of both Yildirim Beyazit University Medical School and Bilkent University. We received informed permission from all the blood donors. We acquired 3 ml intravenous whole blood from each volunteer into vacuum tubes containing 3.2% sodium citrate anticoagulant at most 6 h before the tests. The samples were incubated at 37 °C before use. Thromborel S Human Thromboplastin was purchased from Siemens as the coagulation activator reagent. 47.5 mg Thromborel S Human Thromboplastin was dissolved in 250 µl DI water at room temperature. 10 µl of the solution was pipetted into the inlet of the sample channel of each cartridge, and the cartridges were left at −80 °C for 2 h. The reagents in the cartridges were then lyophilized in a freeze-dryer (Labconco, US) for 6 h, and the cartridges were stored at 4 °C until their use.

Citric acid and sodium bicarbonate were purchased from Sigma-Aldrich and stored at room temperature. Coverslips (20 mm x 20 mm, thickness: 0.15 mm) were purchased from neuVitro. Silicone (ID: 1/32 in. and tygon (ID: 3/32 in. tubings were purchased from Cole Parmer. Blood lancet was purchased from Hema-Lab Ltd. Dual bulb exact volume pipettes (50 µl) were purchased from Alpha Laboratories Ltd. Liquid sodium citrate as an anticoagulant was passed through the exact volume pipettes, and the pipettes were left to dry at room temperature overnight.

2.2. Cartridge fabrication

The test cartridge design was drawn in a CAD software (Autodesk, AutoCAD 2016). Transparent 3 mm thick polmethyl methacrylate (PMMA) sheet was obtained from a local supplier, and the cartridges were fabricated out of PMMA using a 30 W CO_2 laser cutter (Epilog, Zing) [34]. The feed rate, power, and frequency of the cutter were set to 2.6 cm/s, 2.4 W, and 1000 Hz, respectively. The cartridge has a 34 mm x 127 mm rectangular structure. It has two inlets for two separate serpentine channels. One channel is for the reference fluid (DI water), and the other channel is for the sample fluid (whole blood). The inlet chamber volumes are 85 mm^3, and the outlet chamber volume is 16 mm^3. The serpentine channels have 80 µm height and 250 µm width.

The Hagen-Poiseuille law for a steady, laminar, and Newtonian flow states that

$$\Delta P = QR \tag{1}$$

where ΔP is the pressure difference, Q is the volumetric flow rate, and R is the channel resistance [35]. For rectangular channels, the hydrodynamic resistance for $0 < h/w < 1$ is approximated as

$$R = \frac{12\eta L}{wh^3}\left[1-0.63\frac{h}{w}\right]^{-1} \tag{2}$$

where η is the dynamic viscosity, L is the channel length, w is the channel width, and h is the channel height. Also,

$$Q = \frac{wh\,\Delta L}{\Delta t} \tag{3}$$

where t is the time. Plugging Eqs. (2) and (3) into Eq. (1), we have

$$L = \sqrt{\frac{th^2\Delta P}{12\eta}\left[1-0.63\frac{h}{w}\right]} \tag{4}$$

DI water dynamic viscosity is lower than whole blood apparent viscosity, so the water flows faster in a channel in a given time interval [36]. Therefore, the length of the serpentine channels is found by taking the water flow into consideration. The clotting time for a whole blood sample is around 110 s at max. The channel length should be sufficiently long so that water does not reach the outlet until the coagulation, i.e., $t = 110\,s$. ΔP generated by the effervescent pump is $195\,mbar$ as explained in the next section. Also, $h = 80\,\mu m$ and $\eta = 8.9x10^{-4}\,Pa.\ s$. Plugging these parameters in Eq. (4), the length of the serpentine channel is calculated as 1100 mm.

2.3. Effervescent pump fabrication

The effervescent pump consists of four polymer layers and a coverslip as shown in Fig. 1. The four layers were designed in a CAD software (SolidWorks 2016) and fabricated by a 3D-printer (M200, Zortrax) with 100% infill. The filament was acrylonitrile butadiene styrene (ABS), a thermoplastic polymer used as a

common 3D printing material [37]. The 1st printed layer contains a

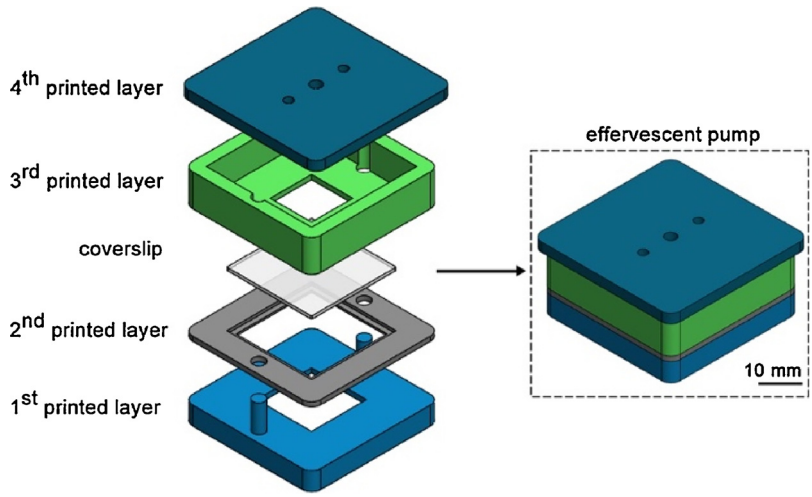

Fig. 1. Schematic drawing of the effervescent pump layers and their assembly. The pump has four 3D-printed layers and a glass coverslip. The 1st and 3rd layers contain the aqueous solution and acid powder, respectively.

space for aqueous solution filling and two posts for the alignment of the other layers. Following the filling of the aqueous solution (1 ml DI water and dissolved base), the 2nd printed layer is aligned on top of the 1st printed layer. Afterwards, a glass coverslip with 150 µm thickness is fit in the 2nd printed layer. Then, the 3rd printed layer is aligned on top of the 2nd printed layer. This layer contains a window in contact with the coverslip where we add the acid powder. The 4th printed layer contains a hole at the center for the insertion of a metal pin and two identical holes for the insertion of tubings. The other ends of these tubings are later inserted to the inlets of the cartridge. A metal pin is covered with a gasket made of soft silicone tubing to prevent gas leakage, and the pin is inserted to the center hole of the 4th layer. Following the insertion, a U-shape PMMA bowl was sealed to the pin bottom. This bowl aims to cover the powder on the coverslip such that any orientation change of the pump does not spread the powder. It also ensures that all the powder falls into the aqueous solution after the coverslip breaking. Following the sealing of the bowl to the pin, we placed the 4th layer on top of the 3rd layer. After the alignment of all, the layers are sealed to one another with epoxy adhesive (Pattex, Henkel) to prevent potential leakage. The pump was then tested up to 250 mbar, and no gas leakage was observed.

2.4. Measurement platform

Referring to Eq. (4), the time at which fluid travels a certain distance in a microfluidic channel can be measured once the fluid viscosity, channel dimensions, and applied pressure are known. Using this principle, we aimed at measuring the prothrombin time of a whole blood sample travelling in a microfluidic channel. However, blood is a non-Newtonian fluid, and blood viscosity varies for everyone, depending on various hematological and external parameters such as hematocrit, plasma proteins' concentration, erythrocyte aggregation, and temperature [36,38]. Two different whole blood samples might have the same PT value, but this does not necessarily mean that these samples have the same viscosity. In other words, the quantification of the travel distance of a blood sample is not a correct method for the measurement of PT. Therefore, a reference Newtonian fluid, whose viscosity is constant, is employed along with the whole blood sample for PT measurement. This eliminates the effect of blood viscosity variation on test results.

Fig. 2a and b show the schematic representation and photograph of the device excluding the readout grid. The fabricated pump is tightly placed on the cartridge. There are two gas transfer tubings. Each is a silicone tubing (8 mm), one end of which is inserted to the pump. The

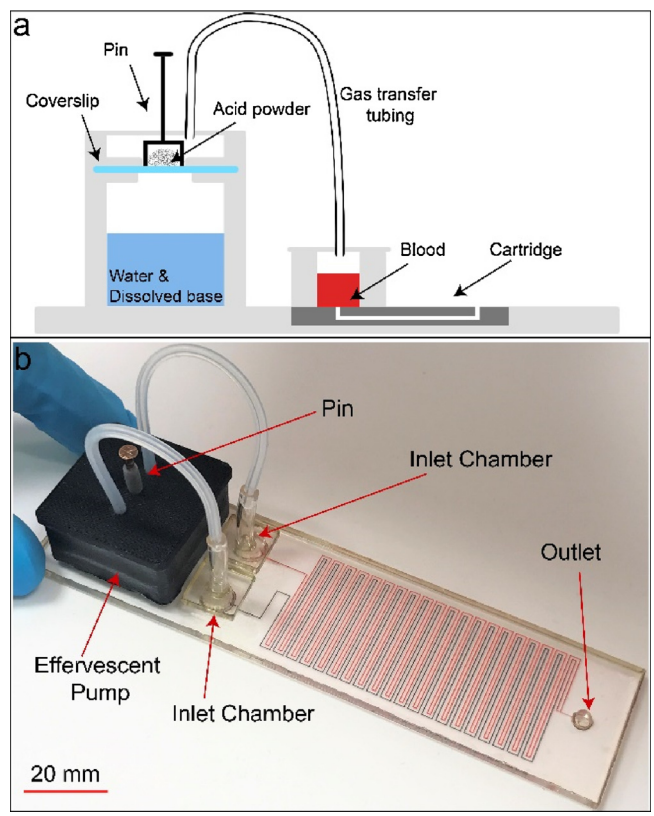

Fig. 2. (a) Schematic representation and **(b)** photograph of the PT measurement device. The device consists of an effervescent pump for CO_2 generation and a two-channel transparent cartridge. Gas pressure drives the sample and reference fluids in their serpentine channels. The coagulation stops the sample fluid flow, and the reference fluid flow is manually stopped at that moment. The distance travelled by the reference fluid is correlated with the sample fluid PT. The fluids used in (b) are DI water coloured with red and black food dyes for demonstration.

other end is inserted to a larger diameter tygon tubing (2 mm) that is inserted to the center hole of a 1 cm x 1 cm PMMA structure. The opposite side of the PMMA structure has a double-sided tape ready for sealing the cartridge inlets. The cartridge has a sample channel (SC) for whole blood and a reference channel (RC) for coloured DI water. The channels share a common outlet. The activator reagent is lyophilized in

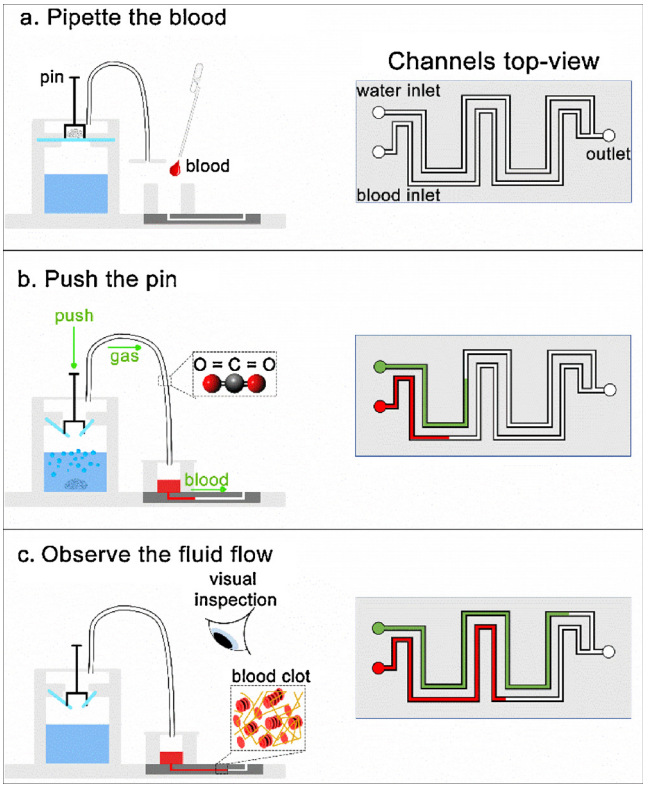

Fig. 3. Schematic representation of the device and the channels while the test is performed. **(a)** The blood sample is pipetted into the SC inlet and mixed with the reagent. **(b)** The pin is pushed, starting the reaction and forming the gas. The generated pressure drives both fluids. **(c)** The blood coagulates, and the fluid flow in the channels is observed by eye.

Table 1
The estimated cost for disposable prothrombin time measurement device.

Material	Dimension/Quantity	Cost (USD)
PMMA substrate	~ 36 cm^2	0.38
ABS polymer	3.2 g	0.16
Glass coverslip	4 cm^2	0.01
Acid, base	0.06 g, 0.2 g	0.001
Pin, tubing, epoxy, tape	–	0.01
Thromborel S activator reagent	1.9 mg	0.48
Total	–	~ **1**

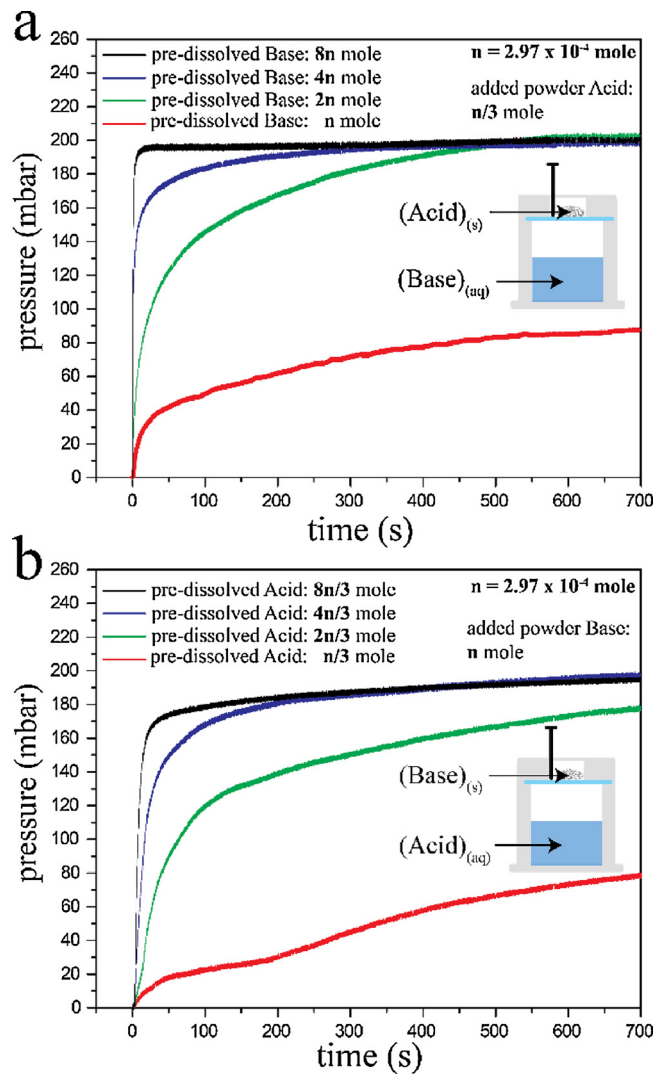

Fig. 4. Characterization of the effervescent pump for different acid and base amounts. The pressure values of CO_2 generated by the reactions were measured. **(a)** Scheme-1: different moles of sodium bicarbonate were dissolved in DI water, and the same mole of citric acid was added to the aqueous solution. **(b)** Scheme-2: different moles of citric acid were dissolved in DI water, and the same mole of sodium bicarbonate was added to the aqueous solution. Scheme-1 allows smaller settling time and longer stay in the equilibrium pressure in 700 s.

the inlet of the SC a few hours before the test (< 6 h). 50 µl DI water is pipetted into the inlet chamber of the RC. Fluidic connections are established between the pump and the channels using tygon tubings.

The following steps are then performed for the measurement:

Step 1. 50 µl anticoagulated whole blood sample is pipetted into the inlet chamber of the SC. The sample is mixed for 5 s with the lyophilized reagent using the pipette to trigger the coagulation process. Then, the PMMA structure is placed on the chamber for the tubing connection between the pump and SC (Fig. 3a). The capillary force or the pressure generated by the placement of the PMMA structure over the inlet does not drive the sample in the serpentine microchannel at this stage due to the channel hydrophobicity.

Step 2. The pump pin is gently pushed down with a finger to break the coverslip (analogous to pressing a START button). The acid powder falls into the aqueous solution, and an acid-base reaction takes place within seconds (Fig. 3b).

Step 3. The generated CO_2 inside the pump and the gas transfer tubings apply equal pressure on the fluids in the inlets (Fig. 3b).

Step 4. This constant pressure drives both the sample and reference fluids in their corresponding channels (Fig. 3b).

Step 5. After some time, the sample fluid stops flowing in the SC due to the coagulation, which forms stable fibrin strands trapping the blood cells and adhering to the SC surfaces (Fig. 3c).

The aim is to measure the distance travelled by the reference fluid using the custom-developed grid when the sample fluid stops flowing (step-5). For this purpose, one of two alternative steps can be performed depending on the user's choice/need.

Step 6. (first alternative) At the instant when the sample fluid stops, the tubing ensuring the connection between the pump and the RC chamber inlet is manually pulled from the corresponding pump hole to prevent further gas transfer. This stops the flow of the reference fluid in the RC. For the clinical tests at the local hospital, we preferred this method and did not experience any difficulty. However, this step might be prone to minor user-mediated error if the user is not attentive enough to stop the reference fluid flow at the right time.

Step 6. (second alternative) Following step-2, a video of the device with the grid underneath is recorded using a cell phone for 3 min. For ease of operation, a custom-made cell phone stand was fabricated out of

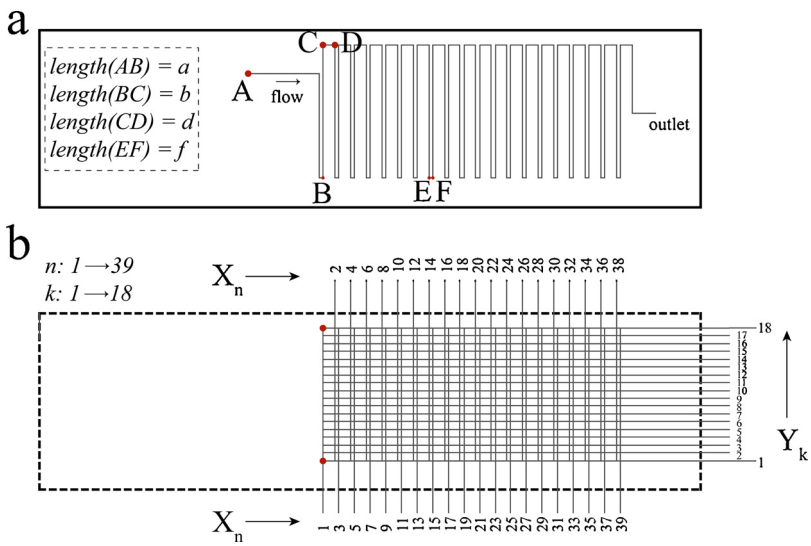

Fig. 5. Grid design for quantitative distance measurement. **(a)** Schematic drawing of the test cartridge demonstrating only the reference channel. **(b)** The grid for the measurement. The dashed lines correspond to the cartridge borders. The grid has 18 horizontal lines *k* and 39 vertical lines *n*.

PMMA using the laser cutter. Then, the video can be replayed to find the frame where the sample fluid stops flowing.

Step 7. The distance travelled by the reference fluid is measured using the grid by naked eye from either the device itself (1st alternative) or from the recorded video (2nd alternative). This distance is a measure of the PT of the sample fluid.

Referring to step-1, 5-s manual mixing of the blood with the reagent seems a drawback in terms of a potential for user-mediated error. A magnet or a pinch valve could have been used for the same purpose. However, we have not integrated such a mechanism to keep the cost lower. To characterize the time error during the mixing, a co-author performed the same 5-s pipette mixing 50 times. At the same time, another co-author employed a timer to measure the time as a reference. The mean and standard deviation of the repetitive tests are 5.28 s and 0.44 s, respectively. Similarly, we asked 50 different volunteers (age range: 15–65) to perform a pipette mixing. The mean and standard deviation of these tests are 5.26 s and 0.74 s, respectively. In each case, the error is less than 1 s.

Before proceeding to the pump characterization, it is worth noting that the material cost of the entire device is around a dollar as listed in Table 1.

3. Results and discussion

3.1. Effervescent pump characterization

The neutralization reaction between citric acid ($H_3C_6H_5O_7$) and sodium bicarbonate ($NaHCO_3$) in an aqueous solution yields carbon dioxide (CO_2) and salt [39].

$$H_3C_6H_5O_{7(aq)} + 3NaHCO_{3(aq)} \grave{a} 3CO_{2(g)} + 3H_2O_{(l)} + Na_3C_6H_5O_{7(aq)}$$

We employed the gaseous product of this acid-base reaction as the pumping source to drive the fluids in the channels. To find the optimum concentration of the reactants for which the gas pressure reaches the equilibrium value as fast as possible (i.e., low settling time) and keeps its value during the PT measurement (max 100 s), the pump was characterized with different amounts of the acid and base. The two schemes taken into consideration were (1) dissolving the base powder in DI water and then adding the acid powder and (2) dissolving the acid powder in DI water and then adding the base powder. We have also considered adding the acid and base powders to the water at the same time, but that dramatically increased the settling time.

During the pump construction, we added base dissolved aqueous solution to the 1st layer and the acid powder to the 3rd layer for scheme-1, or acid dissolved aqueous solution to the 1st layer and the base powder to the 3rd layer for scheme-2. After the pump construction, we inserted a metal pin to the center hole and a silicone tubing to one of the side holes of the 4th layer. The other hole was sealed with silicone glue to prevent leakage. The other end of the tubing was connected to a pressure sensor (40PC015 G, Honeywell), which was sampled using a data acquisition card (DAQPad-6015, National Instruments, US). Fig. 4a plots the generated pressure for four different concentrations of the dissolved base when the same acid powder amount (0.99×10^{-4} mole) was used.

Let 0.99×10^{-4} be /3. Referring to the chemical equation, the ratio of the stoichiometric coefficient of the acid to the base is *1/3*. Therefore, at equilibrium, $n/3$ mole of the acid reacts with n mole of base (red signal, Fig. 4a). In this case, the pressure increases at a slow rate, and the equilibrium pressure cannot be reached within 700 s. Then, $2n$, $4n$, and $8n$ moles of the base were dissolved for different pumps. In these cases, the acid is the limiting reactant, so regardless of the increase of the base mole, the generated gas amount is always n mole. On the other hand, increasing the base amount from n mole up to $8n$ mole enhances the interaction between the acid and base molecules, resulting in a significant decrease in the settling time. When $8n$ mole of the base is dissolved (black signal, Fig. 4a), the settling time is 5 s; the equilibrium pressure is 195 mbar and it stays constant for 700 s. For the other base amounts, the settling time differs, but if we wait long enough, the pressure value reaches to the equilibrium (195 mbar) since the generated gas amount is the same.

Similarly, Fig. 4b plots the generated pressure values for four different concentrations of the dissolved acid when the same base powder amount (2.97×10^{-4} mole) was used. Let 2.97×10^{-4} be. At equilibrium, n mole of the base reacts with $n/3$ mole of the acid (red signal, Fig. 4b). We observe that this amount is not enough to reach the equilibrium pressure within 700 s. Therefore, the acid amount was increased to $2n/3$, then $4n/3$, and finally to $8n/3$. In these cases, the base is the limiting reactant, so the generated gas amount is always n mole. As also witnessed in Fig. 4a while increasing the base amount, increasing the acid amount here facilitates the molecular interaction and therefore decreases the settling time. On the other hand, in this scheme, none of the reactions could reach the equilibrium gas pressure within 700 s; only the reaction for $8n/3$ mole of the acid approaches it very closely.

The pressure generated by the chemical reaction reaches to the equilibrium value faster in scheme-1 compared to scheme-2. The pre-dissolved reactant (base in scheme-1 and acid in scheme-2) is always

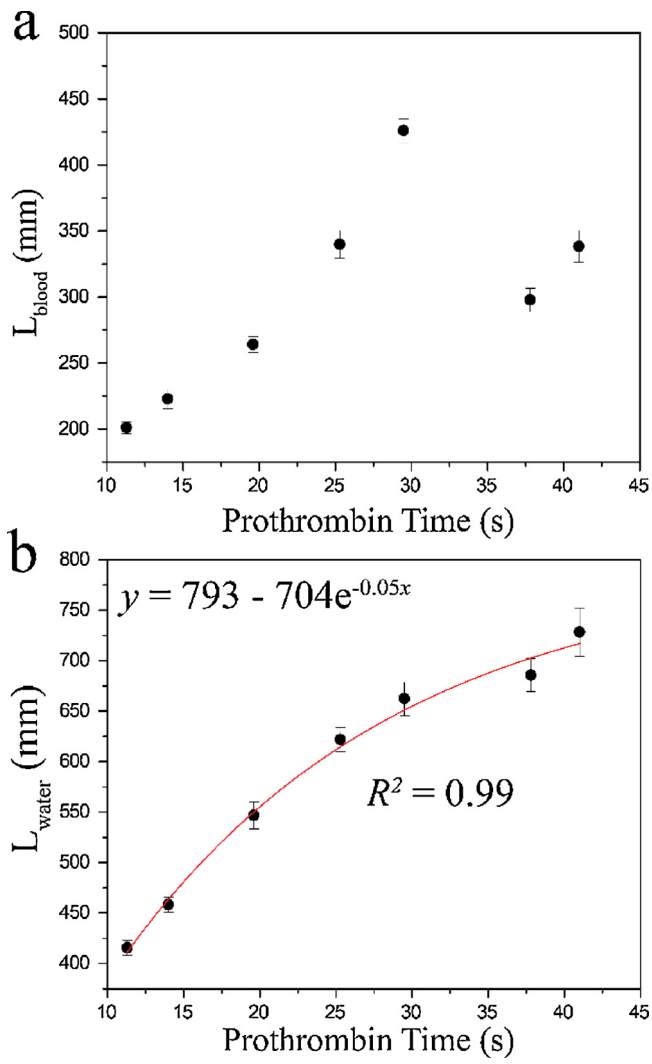

Fig. 6. Comparing the device with the conventional benchtop PT analyser for PT measurement. 7 whole blood samples were tested three times. Error bars indicate 2 standard deviations. (a) Conventional PT measurement versus blood travel distance does not have any correlation due to the differences in blood viscosities. (b) Conventional PT measurement versus water travel distance correlates 99% using the exponential function, ($y = a - b\,e^{-cx}$).

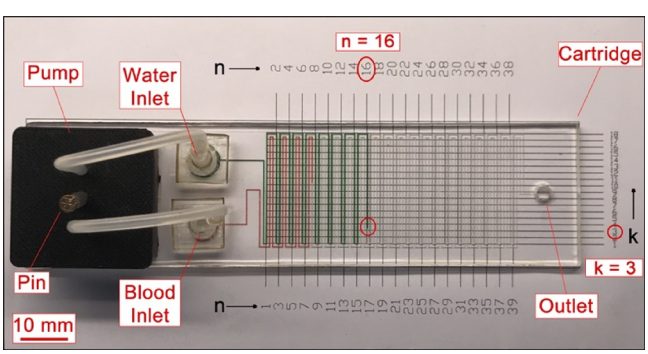

Fig. 7. The photograph of the device after the PT measurement test for the case study. The device is an integrated single-unit and consists of a pump, a cartridge, and a grid. With the coagulation of the blood sample, the green coloured DI water stops at (n, k) = (16, 3), which can be read with naked eye.

ready for the reaction, so it is the reactivity of the reactant added later to the aqueous solution that causes this difference. In scheme-1, the added reactant is citric acid whose ionization/dissociation constant is higher than that of the sodium bicarbonate (like the case for many other acids compared to bases) [39]. The reaction starts faster, and therefore the equilibrium pressure is reached faster. Based on these observations, scheme-1 was chosen for the pump of the device. 8*n*mole of sodium bicarbonate was dissolved in DI water, and n mole of citric acid was placed onto the coverslip whose breakage with the metal pin would start the reaction.

3.2. Quantitative distance measurement

The measurement principle of the device is based on the assessment of the distance travelled by the reference liquid in its corresponding channel (RC) at the end of the coagulation process. Since there is no electronic readout unit for the device, which indeed makes it low-cost and disposable, accurate quantitative distance measurement with the naked eye is essential. Therefore, we designed a grid specific for the test cartridge. Fig. 5a is the schematic drawing of the cartridge demonstrating only the RC. Point A is where the flow starts from the inlet. Fig. 5b is the designed grid where the dashed lines correspond to the borders of the cartridge. Point B in Fig. 5a matches with the bottom red point in Fig. 5b. The grid consists of 18 horizontal (k) and 39 vertical (n) lines. The distance between two horizontal lines is 1.5 mm. The vertical lines are divided into two sets: odd (written bottom) and even (written top). The distance between two odd vertical lines and between two even vertical lines is 2.25 mm.

The grid was drawn in a CAD software (Autodesk, AutoCAD 2016) and printed on a white paper. Then, the printed paper was taped on a PMMA layer (thickness: 3 mm, width: 8 mm, length: 15 mm). The cartridge is placed on the paper grid such that the cartridge stays inside the representative cartridge borders of the paper grid (dashed lines in Fig. 5b). The liquid flow starts with the start of the chemical reaction and ends with the blood coagulation. Following the coagulation, it is read with naked eye to determine the vertical (n) and horizontal line (k) at which the reference liquid has stopped.

If n is odd, the travelled distance is calculated using the following equation,

$$L_{nk} = 0.75\,[10 + 36n + 2k]\ mm \tag{5}$$

If n is even, the travelled distance is calculated using the following equation,

$$L_{nk} = 0.75\,[45 + 36n - 2k]\ mm \tag{6}$$

where {n | 1 ≤ n ≤ 39} and {k | 1 ≤ k ≤ 18}. It is also possible that the liquid may stop between two *n* or two *k* values. In this case, the user can decide which value to choose. The error will be less than 1.5 mm, which corresponds to 0.1 s error in PT.

3.3. Comparative prothrombin time tests

We performed tests at a clinic to demonstrate the correlation between the reference fluid travel distance measured from the device and the conventionally measured PT time. Human thromboplastin was lyophilized in the sample inlets of the cartridges. The donor whole blood samples were acquired via venipuncture into blood tubes. The tubes were centrifuged to get the plasma portion which was then placed into the benchtop PT analyzer (Sysmex, Siemens). Following the conventional PT measurement, 7 whole blood samples whose PT values were between 10 s and 45 s were picked from the sample population (healthy range is: 10–17 s). Afterwards, we introduced 50 µl from a whole blood sample into the sample inlet of a cartridge for a single test. Each blood sample was tested three times. The distances travelled by the sample and the coloured DI water were measured using the Eqs. (5) and (6).

Fig. 6 demonstrates the regression analysis for the correlation between the conventionally measured PT versus the distance travelled by the sample fluid (Fig. 6a) and the distance travelled by the reference

Table 2
A portion of the n-by-k table tabulating the prothrombin time values (in seconds), for the healthy population range.

n k	1	2	**3**	4	5	6	7	8	9	10	11	12	13	14	15	16	17	18
12	9.55	9.48	9.41	9.34	9.28	9.21	9.14	9.07	9.01	8.94	8.87	8.81	8.74	8.67	8.61	8.54	8.48	8.41
13	9.72	9.79	9.86	9.93	10.00	10.07	10.14	10.21	10.28	10.35	10.43	10.50	10.57	10.64	10.72	10.79	10.86	10.93
14	12.19	12.11	12.03	11.95	11.88	11.80	11.72	11.65	11.57	11.49	11.42	11.34	11.27	11.19	11.12	11.05	10.97	10.90
15	12.38	12.46	12.54	12.62	12.70	12.78	12.87	12.95	13.03	13.11	13.19	13.28	13.36	13.44	13.52	13.61	13.69	13.78
16	15.23	15.14	**15.05**	14.96	14.87	14.78	14.69	14.60	14.51	14.42	14.34	14.25	14.16	14.08	13.99	13.91	13.82	13.74
17	15.46	15.55	15.64	15.74	15.83	15.93	16.02	16.12	16.21	16.31	16.40	16.50	16.60	16.70	16.80	16.89	16.99	17.09
18	18.82	18.71	18.60	18.49	18.39	18.28	18.17	18.07	17.96	17.86	17.76	17.65	17.55	17.45	17.35	17.24	17.14	17.04

fluid (Fig. 6b). No correlation can be seen between the conventional PT and the distance travelled by the sample fluid. Referring to Eq. (4), the viscosity values of the sample fluids are also in play, determining the flow characteristics of the fluids along with their coagulation times. This finding has also rationalized the use of the reference fluid having the same viscosity across the tests. On the other hand, the correlation coefficient between the conventional PT values and the distance travelled by the reference fluid is 99% using the following exponential decay function $y = a - b\,e^{-cx}$ where $a = 793$, $b = 704$, and $c = 0.05$. This trend shows that as the PT value increases, the distance travelled by the water also increases but at a decreasing rate each time. Referring to Eq. (2), the reason for the decreasing rate is the increase in the resistance, R, of the channel as the fluid proceeds within the channel (as L increases). The increase in the resistance makes it difficult for the fluid to flow, delaying its progress.

According to Fig. 6b, the equation relating the PT (T) to the travelled distance (L_{nk}) is the following:

$$T = 20\,ln\left[\frac{704}{793 - L_{nk}}\right] s \tag{7}$$

To free the user from any mathematical calculations, we have prepared a table tabulating the prothrombin time values (T) for any n and k.

3.4. Personal prothrombin time measurement

The aim of this entirely disposable device is to allow facile PT measurement from fingerprick blood for home use by the patients. We therefore carried out a case study to demonstrate the potential of the device toward this goal. (I) The pump having the chemicals, pin, and tubings, (II) the cartridge having the green coloured DI water in the reference inlet and lyophilized reagent in the sample inlet, and (III) the paper grid are all integrated together to make the device a single-unit. A test kit was prepared that has a blood lancet, an exact volume pipette (the pipette interior is anticoagulated – see Materials), and the device. The kit was handed to a 65-year old female volunteer who has been undertaking anticoagulant therapy and using Coumadin® for 10 years. Verbal instructions were given to her who performed the steps herself. The left middle finger was punched using the blood lancet. 50 µl whole blood was taken into the exact volume pipette and then introduced the sample inlet. Following 5 s gentle mixing of the sample with the pipette, the inlet was sealed with the square PMMA structure to establish the tubing connection. The pin of the pump was gently pushed to start the reaction. The whole blood flow was observed, and when it stopped, the pump side of the tubing, which transfers gas to the water inlet, was manually disconnected from the pump. This immediately stopped the water flow. Then, the intersection of the vertical and horizontal lines of the grid was read with the eye without any difficulty. The vertical line was the 16th (n = 16) and the horizontal line was the 3rd (k = 3) as shown in Fig. 7. Since n is even, Eq. (6) gives the distance travelled by the water, which is $L_{nk} = 461.25\,mm$. The prepared table was used to find the prothrombin time for these n and k values as *15.05 s* (marked red in Table 2). The volunteer is asked to repeat the test 5 times in total over the course of one hour. The mean and the standard deviation of the measured PT are *14.45 s* and *0.44 s*, respectively. The fingerprick whole blood of the same volunteer was also tested with Hemochron® Signature Elite (Accriva) as a reference, and the PT was measured as 14 s, which agrees well with the result of the presented device.

The physicians can sometimes be suspicious about the potential of the home-use of the point-of-care devices for two primary reasons [26]. (I) The patient might get an erroneous diagnostic result or no result at all due to wrong use of the device. (II) The patient might get the correct diagnostic result but take a wrong action based on the result such as changing the dose of a medicine. The developed device can still comfortably be used as a telemedicine platform even if these concerns are present. The test results or the video of the tested cartridge can be shared with a professional for the evaluation of the test result. This eliminates both the wrong use of the device as well as discouraging the user to take actions before informing the physician.

Viscosity of coagulating or non-coagulating whole blood is another clinically relevant parameter, which is often overlooked. The determination of average blood viscosity during coagulation is important to understand the interrelation between coagulation dynamics and hemorheological properties [40,41]. The viscosity of blood is affected by shear rate due to two distinct internal mechanisms that yields its non-Newtonian characteristics: erythrocyte aggregation and erythrocyte deformation [38,42,43]. Thus, it is critical to perform the coagulation time measurements at physiologically relevant flow conditions. The presented double channel structure with a reference flow channel is a potential platform for such a measurement. Since the reference flow viscosity is known, the coagulating sample viscosity can be measured, which has clinical value rather than home-use. Then, as a future direction, the disposable platform can be used for obtaining the two parameters – PT and viscosity simultaneously from the same blood sample.

4. Conclusion

We presented a portable and entirely disposable device enabling point-of-care prothrombin time measurement from 50 µl whole blood in less than 2 min. This device consists of the full integration of an effervescent pump, a two-channel test cartridge, and a grid for readout. The use of the effervescent pump, carrying out a neutralization reaction to generate CO_2 for fluid handling, eliminates the need of external components for pumping and energy source. Also, the custom-made paper grid allows easy readout with naked eye, freeing the system from a costly readout unit. The underlying principle is based on the measurement of the distance travelled by the reference fluid in a serpentine channel, right after the coagulation process of the sample fluid in the other serpentine channel of the cartridge. The test results performed at a local hospital demonstrated the high correlation between the conventionally measured PT and the reference fluid travel distance. The case study revealed the ease-of-use of the device by non-professionals for home use and showed the potential of the device for coagulation screening at the point-of-care. This portable, low-cost, lightweight, disposable, easy-to-use and rapid device is promising for periodic PT measurement from low volume whole blood for both lab- and home-based monitoring.

Acknowledgements

The authors thank Prof. Ozcan Erel for the clinical tests and Dr. Ismail Bilican for the comments on the manuscript. Ziya Isiksacan is supported by ASELSAN Graduate Scholarship for Turkish Academicians. The authors acknowledge support from The Scientific and Technologic Research Council of Turkey (TUBITAK project no. 213S127).

References

[1] B. Furie, B.C. Furie, The molecular basis of blood coagulation, Cell 53 (1988) 505–518, http://dx.doi.org/10.1016/0092-8674(88)90567-3.
[2] J.S. Flier, L.H. Underhill, B. Furie, B.C. Furie, Molecular and cellular biology of blood coagulation, N. Engl. J. Med. 326 (1992) 800–806, http://dx.doi.org/10.1056/NEJM199203193261205.
[3] J. Antovic, M. Blombäck, Essential Guide to Blood Coagulation, John Wiley & Sons, 2013.
[4] M. Hoffman, Remodeling the blood coagulation Cascade, J. Thromb. Thrombolysis. 16 (2003) 17–20, http://dx.doi.org/10.1023/B:THRO.0000014588.95061.28.
[5] J.L. Hood, C.S. Eby, Evaluation of a prolonged prothrombin time, Clin. Chem. 54 (2008) 765–768, http://dx.doi.org/10.1373/clinchem.2007.100818.
[6] P. Toulon, Y. Ozier, A. Ankri, M.-H. Fléron, G. Leroux, C.M. Samama, Point-of-care versus central laboratory coagulation testing during haemorrhagic surgery. A multicenter study, Thromb. Haemost. 101 (2009) 394–401, http://dx.doi.org/10.1160/TH08-06-0383.
[7] S.A. Kozek-Langenecker, Perioperative coagulation monitoring, Best Pract. Res. Clin. Anaesthesiol. 24 (2010) 27–40, http://dx.doi.org/10.1016/j.bpa.2009.09.009.
[8] K. Harter, M. Levine, S.O. Henderson, Anticoagulation drug therapy: a review, West. J. Emerg. Med. 16 (2015) 7–11, http://dx.doi.org/10.5811/westjem.2014.12.22933.
[9] M. Franchini, G.M. Liumbruno, C. Bonfanti, G. Lippi, The evolution of anticoagulant therapy, Blood Transfus. 14 (2016) 175–184, http://dx.doi.org/10.2450/2015.0096-15.
[10] J. Hirsh, J. Dalen, D.R. Anderson, L. Poller, H. Bussey, J. Ansell, D. Deykin, Oral anticoagulants: mechanism of action, clinical effectiveness, and optimal therapeutic range, Chest 119 (2001) 8S–21S.
[11] B. Collins, C. Hollidge, Antithrombotic drug market, Nat. Rev. Drug Discov. 2 (2003) 11–12, http://dx.doi.org/10.1038/nrd966.
[12] D.B. Petitti, B.L. Strom, K.L. Melmon, Duration of warfarin anticoagulant therapy and the probabilities of recurrent thromboembolism and hemorrhage, Am. J. Med. 81 (1986) 255–259, http://dx.doi.org/10.1016/0002-9343(86)90260-3.
[13] C.S. Landefeld, R.J. Beyth, Anticoagulant-related bleeding: clinical epidemiology, prediction, and prevention, Am. J. Med. 95 (1993) 315–328, http://dx.doi.org/10.1016/0002-9343(93)90285-W.
[14] V. Gubala, L.F. Harris, A.J. Ricco, M.X. Tan, D.E. Williams, Point of care diagnostics: Status and future, Anal. Chem. 84 (2012) 487–515, http://dx.doi.org/10.1021/ac2030199.
[15] W.S. Baker, K.J. Albright, M. Berman, H. Spratt, P.A. Mann, J. Unabia, J.R. Petersen, Clinica chimica acta POCT PT INR — Is it adequate for patient care? A comparison of the Roche coaguchek XS vs. Stago star vs. Siemens BCS in patients routinely seen in an anticoagulation clinic, Clin. Chim. Acta 472 (2017) 139–145, http://dx.doi.org/10.1016/j.cca.2017.07.027.
[16] L.F. Harris, V. Castro-Lopez, A.J. Killard, Coagulation monitoring devices: past, present, and future at the point of care, TrAC - Trends Anal. Chem. 50 (2013) 85–95, http://dx.doi.org/10.1016/j.trac.2013.05.009.
[17] C.M. Lehman, Instrumentation for the coagulation laboratory, Lab. Hemost. Springer International Publishing, Cham, 2015, pp. 33–43, http://dx.doi.org/10.1007/978-3-319-08924-9_3.
[18] B. Ramaswamy, Y.T. Yeh, S. Zheng, Microfluidic device and system for point-of-care blood coagulation measurement based on electrical impedance sensing, Sens. Actuators B Chem. 180 (2013) 21–27, http://dx.doi.org/10.1016/j.snb.2011.11.031.
[19] T.M.A. Gronewold, S. Glass, E. Quandt, M. Famulok, Monitoring complex formation in the blood-coagulation cascade using aptamer-coated SAW sensors, Biosens. Bioelectron. 20 (2005) 2044–2052, http://dx.doi.org/10.1016/J.BIOS.2004.09.007.
[20] H. Li, D. Han, G.M. Pauletti, A.J. Steckl, Blood coagulation screening using a paper-based microfluidic lateral flow device, Lab Chip 14 (2014) 4035–4041, http://dx.doi.org/10.1039/C4LC00716F.
[21] O. Cakmak, E. Ermek, N. Kilinc, S. Bulut, I. Baris, I.H. Kavakli, G.G. Yaralioglu, H. Urey, A cartridge based sensor array platform for multiple coagulation measurements from plasma, Lab Chip 15 (2015) 113–120, http://dx.doi.org/10.1039/C4LC00809J.
[22] M. Andersson, J. Andersson, A. Sellborn, M. Berglin, B. Nilsson, H. Elwing, Quartz crystal microbalance-with dissipation monitoring (QCM-d) for real time measurements of blood coagulation density and immune complement activation on artificial surfaces, Biosens. Bioelectron. 21 (2005) 79–86, http://dx.doi.org/10.1016/j.bios.2004.09.026.
[23] C.-H. Lin, C.-Y. Liu, C.-H. Shih, C.-H. Lu, A sample-to-result system for blood coagulation tests on a microfluidic disk analyzer, Biomicrofluidics 8 (2014) 52105, http://dx.doi.org/10.1063/1.4893917.
[24] M.M. Dudek, N. Kent, K.M. Gustafsson, T.L. Lindahl, A.J. Killard, Fluorescence-based blood coagulation assay device for measuring activated partial thromboplastin time, Anal. Chem. 83 (2011) 319–328, http://dx.doi.org/10.1021/ac102436v.
[25] G.M. Whitesides, The origins and the future of microfluidics, Nature 442 (2006) 368–373, http://dx.doi.org/10.1038/nature05058.
[26] Z. Isiksacan, M.T. Guler, A. Kalantarifard, M. Asghari, C. Elbuken, Lab-on-a-chip platforms for disease detection and diagnosis, Biosens. Nanotechnol. (2017) 155–181, http://dx.doi.org/10.1002/9781119065036.ch8 John Wiley & Sons, Inc., Hoboken, NJ, USA.
[27] D.J. Laser, J.G. Santiago, A review of micropumps, J. Micromech. Microeng. 14 (2004) R35–R64, http://dx.doi.org/10.1088/0960-1317/14/6/R01.
[28] A.K. Au, H. Lai, B.R. Utela, A. Folch, Microvalves and micropumps for BioMEMS, Micromachines 2 (2011) 179–220, http://dx.doi.org/10.3390/mi2020179.
[29] C. Zhou, H. Zhang, Z. Li, W. Wang, Chemistry pumps: a review of chemically powered micropumps, Lab Chip 16 (2016) 1797–1811, http://dx.doi.org/10.1039/C6LC00032K.
[30] T.R. Kline, W.F. Paxton, Y. Wang, D. Velegol, T.E. Mallouk, A. Sen, Catalytic micropumps: microscopic convective fluid flow and pattern formation, J. Am. Chem. Soc. 127 (2005) 17150–17151, http://dx.doi.org/10.1021/JA056069U.
[31] A.A. Farniya, M.J. Esplandiu, D. Reguera, A. Bachtold, Imaging the proton concentration and mapping the spatial distribution of the electric Field of catalytic micropumps, Phys. Rev. Lett. 111 (2013) 168301, , http://dx.doi.org/10.1103/PhysRevLett.111.168301.
[32] J.P. Esquivel, M. Castellarnau, T. Senn, B. Löchel, J. Samitier, N. Sabaté, Fuel cell-powered microfluidic platform for lab-on-a-chip applications, Lab Chip 12 (2012) 74–79, http://dx.doi.org/10.1039/C1LC20426B.
[33] B.T. Good, C.N. Bowman, R.H. Davis, An effervescent reaction micropump for portable microfluidics system, Lab Chip 6 (2006) 659–666, http://dx.doi.org/10.1039/B601542E.
[34] Z. Isiksacan, M.T. Guler, B. Aydogdu, I. Bilican, C. Elbuken, Rapid fabrication of microfluidic PDMS devices from reusable PDMS molds using laser ablation, J. Micromech. Microeng. 35008 (9) (2016), http://dx.doi.org/10.1088/0960-1317/26/3/035008.
[35] F.M. White, Fluid Mechanics, McGraw Hills, 2010.
[36] O.K. Baskurt, Handbook of Hemorheology and Hemodynamics, IOS Press, 2007.
[37] C. Schubert, M.C. van Langeveld, L.A. Donoso, Innovations in 3D printing: a 3D overview from optics to organs, Br. J. Ophthalmol. 98 (2014) 159–161, http://dx.doi.org/10.1136/bjophthalmol-2013-304446.
[38] Z. Isiksacan, M. Asghari, C. Elbuken, A microfluidic erythrocyte sedimentation rate analyzer using rouleaux formation kinetics, Microfluid. Nanofluidics 21 (44) (2017), http://dx.doi.org/10.1007/s10404-017-1878-7.
[39] R.H. Perucci, F.G. Herring, J.D. Madura, C. Bissonnette, General Chemistry: Principles and Modern Applications, Pearson Prentice Hall, 2010.
[40] M. Ranucci, T. Laddomada, M. Ranucci, E. Baryshnikova, Blood viscosity during coagulation at different shear rates, Physiol. Rep. 2 (2014) e12065, http://dx.doi.org/10.14814/phy2.12065.
[41] E. Yeom, J.H. Park, Y.J. Kang, S.J. Lee, Microfluidics for simultaneous quantification of platelet adhesion and blood viscosity, Sci. Rep. 6 (2016) 24994, http://dx.doi.org/10.1038/srep24994.
[42] Z. Isiksacan, O. Erel, C. Elbuken, A portable microfluidic system for rapid measurement of erythrocyte sedimentation rate, Lab Chip 16 (2016) 4682–4690, http://dx.doi.org/10.1039/C6LC01036A.
[43] M. Kaibara, Rheology of blood coagulation, Biorheology 33 (1996) 101–117, http://dx.doi.org/10.1016/0006-355X(96)00010-8.

Mustafa Tahsin Guler is a post-doctoral research associate at Kirikkale University. He received his M.S. and pH.D. from Kirikkale University (Turkey). His research interests are in the field of microfluidics, rapid prototyping, and medical diagnostics.

Ziya Isiksacan is a pH.D. candidate at the UNAM Materials Science and Nanotechnology Program at Bilkent University. He received his M.S. from The University of Edinburgh (UK). His research interests are in the field of microfluidics, optofluidics, point-of-care diagnostics, and bioelectronics.

Murat Serhatlioglu is a pH.D. candidate at the UNAM Materials Science and Nanotechnology Program at Bilkent University. His research interests are in the field of flow cytometry, microfluidics, femtosecond laser processing, and MEMS.

Caglar Elbuken is an Assistant Professor at Bilkent University, National Nanotechnology Research Center. His research interests include lab-on-a-chip devices, droplet microfluidics, and sensing technologies for portable applications.